HYDRODYNAMIC PERFORMANCE OF SCULLING PROPULSION SYSTEM

M. A. Kotb

Department of Naval Architecture and Marine Engineering
Faculty of Engineering, Alexandria University, Alexandria, Egypt.
E-mail: Abbas@alex.eun.eg

ABSTRACT

Performance of sculling propulsion system was studied using single pass multiple streamtube theory combined with blade element analysis. Actual profile lift and drag data covering full range of incidence and wide range of Reynolds number were used. The analysis was applied to a simple, one bladed sculling propulsion system. Global quantities such as thrust, side force, power, and efficiency are obtained as functions of speed and pitch ratios. Distributions of flow incidence, velocities and elemental forces through blade travel were also examined.

Keywords: Hydrodynamic propulsion, Sculling, Airfoils, Propellers, Blade Performance

NOMENCLATURE

A	wing total planform area (m^2)
a	axial induced velocity factor
b	wing semi span (m)
c	wing chord (m)
CL	sectional lift coefficient C_L
CD	sectional drag coefficient C_D
dF_x	element axial force (N)
dF_t	element side force (N)
dP	element power (W)
G	function given by Equation 9
h	wing span (m)
N	number of blades
N_t	number of time intervals
N_s	number of blade elements
P	power (W)
R_e	Reynolds number
T	Propeller thrust (N)
V_S	ship speed (m/s)
V	axial flow at the wing (m/s)
V_R	resultant velocity to the blade(m/s)
V_t	transverse wing speed (m/s)
V_{tmax}	maximum transverse speed (m/s)
V_∞	undisturbed free stream velocity (m/s)
α	angle of attack to the blade element (deg)
β	flow angle relative to y axis (deg)
η	propeller efficiency (m^2/s)
ν	water kinematics viscosity (kg/m^3)
ρ	water specific density
θ	blade setting angle relative to y axis(deg)

INTRODUCTION

Thrust producing devices for ship propulsion can be classified in a number of ways. Fixed surfaces such as sails are used to generate propelling force from the wind. Rotating devices are more common in the form of propellers that may be horizontally, or verticall mounted. Impellers of water jet engines. Oscillating surfaces can also be used to generate apropelling force, even though they are more commonly used as control surfaces for maneuvering purposes, such as rudders, roll stabilizers, etc. the simplest oscillators used for producing propelling action are oars. Propulsion systems involving oscillating motion have been used in nature by many sea creatures. These creatures use variations of oscillating blades or fins, either as a main propulsion device or as an auxiliary. They employ these devices in many ways. Typical motion includes rowing, flapping and sculling.

Rowing is the method used by most amphibians since it bears the closest resemblance to walking. It involves a fore and aft motion of fins, flippers, or feet combined with feathering. It is also used by many

creatures dwelling at the bottom of lakes, rivers, and the ocean, where again it is probably related to walking.

Flapping fin propulsion consists of a side to side motion of a vertical fin or a tail. The technique is also related to maneuvering and stability control of many fishes.

Sculling is another form of rowing, where transverse motion of the fins is coupled with a synchronized angling of the fins. This is a more efficient use of the fin since propulsive power is obtained in both directions of motion, a mechanism imitating this motion was patented in 1854 by A. Billford of London. A ship was sculled forward by means of port and starboard paddles. The motion of the paddles resembled that of the oars of ancient galleys. That is, the principal oscillation of the paddle shaft was outboard and inboard. Other trials employing oscillating surfaces for propulsion were made by Fowels, Johnson, and Curry [1]. Few studies have been made on sculling propulsion systems. Potze, [2] studied the optimum motion of the wings comprising a sculling propulsion system in order to find the highest possible efficiency and the angle of incidence that will achieve this maximum efficiency for a prescribed mean thrust. Sparenberg and Vries [3] studied the performance of a sculling propulsion system made of two elastically coupled profiles. Sijtsma and Sparenberg, [4] numerically investigated induced drag on sculling propellers to find optimum wingplan form.

Currently, (May 1997), a 3.7 m boat with an oscillating foils, attached to its stern is being tested at the Massachusetts Institute of Technology (MIT) by Prof. Triantafyllou through a project supported by the ONR. The propulsion system tested reached up to 87 percent efficiency. The boat, which measures 3.7* 0.45 m is a scale model of afast ship. Two large motors allow the wings to move toward and away from each other, two smaller motors allow them to twist slightly as they do so. A specific flapping motion of the flippers is programmed aiming at determining the most efficient one. Tests also plan to examine the flippers wake and to design a system that allows for maneuvering , as well as propulsion. Full test results have not been published yet. [5]. Sculling type of propulsion has certain advantages over a conventional screw propeller. Its efficiency is expected to be greater than the efficiency of a screw propeller because the volume of water influenced by the wings can be made larger than the volume of water influenced in general by a screw propeller..Another advantage of the wings with respect to the water is constant over their span, while the velocity of a screw propeller blade increases toward the tip. Of course, a disadvantage is the complexity of the mechanism needed to move the wings.

Sculling propulsion system consists of one or two wings, mounted vertically behind a ship, and which move sideways back and forth. The angles of incidence of the wings are adjusted so that a propelling force is delivered. For practical purposes two wings are appropriate because inconvenient moments acting on the ships can be reduced to a minimum.

Also, the efficiency that obtainable by a propeller with one wing. A schematic sketch of sculling propulsion by means of one or two wings mounted vertically behind a ship is shown in Figure 1.

In this paper, a simple hydrodynamic analysis is presented for predicting the performance of sculling propulsion systems. The analysis is applied to a case study. Results pertaining to the performance are reported and discussed.

HYDRODYNAMIC ANALYSIS OF SCULLING PROPULSION SYSTEM

The performance analysis considered here is based on using the streamwise momentum equation that equates the streamwise forces on the airfoil blades to the change in fluid momentum through the propulsor. Incompressible and invisid fluid is assumed. The influence of the ship's hull is also neglected. Computations are performed for a series of streamtube that pass through the propeller plane.

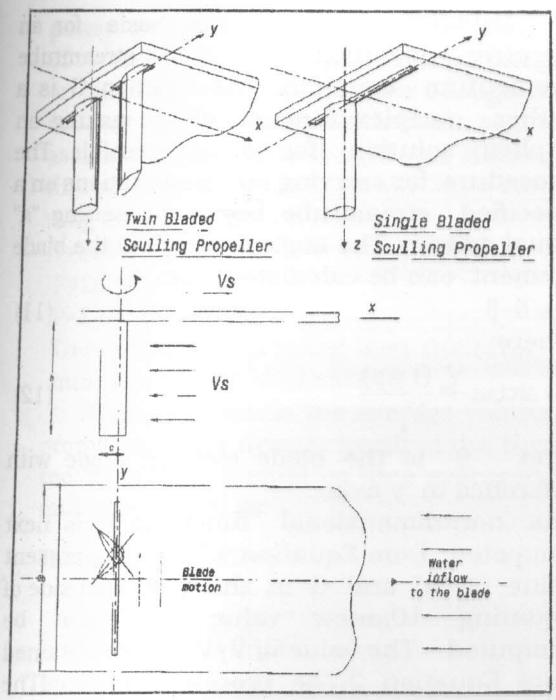

Figure 1 Sculling propulsion systems configuration and coordinate system used

In Figure 2-a a typical streamtube is shown. The cross sectional area of the streamtube is given by $\Delta z\Delta y$ where Δz is the vertical height of the streamtube. The streamtube cross sectional area is assumed to be constant as it passes through the propulsor sweeping plane , although in reality it wil decrease while converging in the downstream direction. The fluid velocity through the streamtube is denoted by and is a function of the position y and z coordinates. Since energy is delivered to the fluid by the blades as they pass through the streamtube, velocity V is greater than the undisturbed velocity . The time averaged streamtube can be used in conjunction with propulsion Equation to relate the velocities V and V_∞ and the average force $\bar{F}_x$ exerted by the blade elements as they pass through the streamtube.

The expression can be written as :

$$\bar{F}_x = 2\rho a(1=a)V_\infty^2 \ \Delta y\Delta z \qquad (1)$$

where

$$\frac{V}{V_\infty} = 1 = a \qquad (2)$$

The average force $\bar{F}_x$ in the streamtube can be related to the streamwise force F_x exerted by an individual blade element as it passes through the streamtube by noting that each of the N blade elements spends $\Delta y/2b$ percentage of their time in the streamtube. Therefore the average force becomes:

$$\bar{F}_X = NF_X\frac{\Delta y}{2b} \qquad (3)$$

In addition, the force Fy , which acts along the blade stroke must be found in order to comp ute the power being required by the element as it passes through the streamtube

A wing element $c\Delta z$ has two velocity components; axial velocity due to ship motion V, and a transverse velocity due to element motion V_T.

The resultant of these two components is V_R where

$$V_R = \sqrt{V^2 = V_1^2} \qquad (4)$$

making an angle with the y axis The oscillating motion of the blade as a function of transverse coordinate y is given by

$$V_1(y) = V_{T\max}\sqrt{1-\left(\frac{y}{b}\right)^2} \qquad (5)$$

A blade at angle θ moves parallel to itself along the y axis. At the end of the stroke, (y = ± b), it reverses direction while turning an angle $\pi-2\theta$ degree around its own axis.

Referring to the blade element velocity diagram and the asslift and drag force components; Figure 2-b we can obtain expressions for blade element forces

F_x and F_y as:

$$F_x=0.5\rho c\Delta z V^2{}_R[C_L\cos\beta-C_D\sin\beta] \qquad (6)$$

$$F_y=0.5\rho c\Delta z V^2{}_R[C_L\sin\beta+C_D\cos\beta] \qquad (7)$$

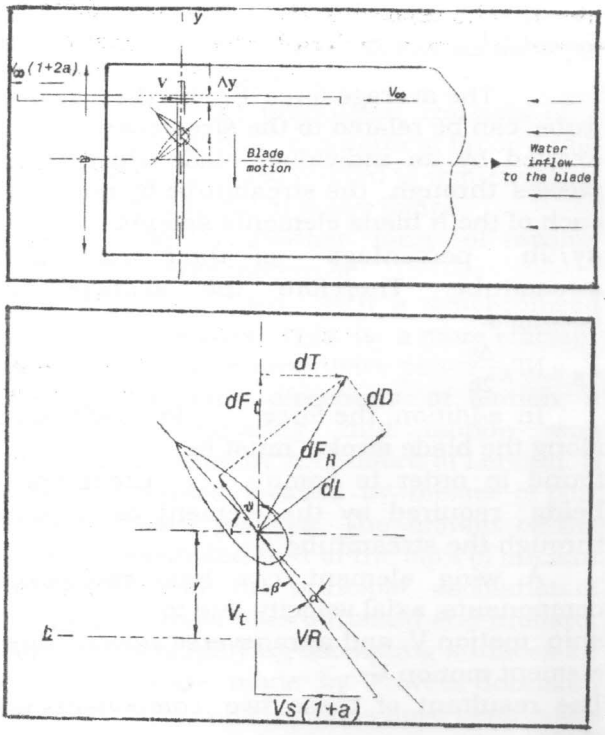

Figure2 sing pass Stream tupe and 2-b Blade Element forces and velocities

where C_L and C_D are lift and drag coefficients of the blade profile used. These are usually functions of both incidence and profile Reynolds number based on the

chord $Re = \frac{cV_R}{\upsilon}$

i.e. $C_L = F_1(\alpha, Re)$ (8a)

$C_D = F_2(\alpha, Re)$ (8b)

where f_1 and f_2 are functions usually obtained through experiments Substituting Equations 1 and 6 into 3 then;

$$2\rho a(1+a)V^2_\infty \Delta y \Delta z = \frac{N\Delta y}{2b} 0.s\rho c \Delta z V^2_R [C_L \cos\beta - C_D sm\beta]$$

which can be reduced to

$$a(1+a) = \left(\frac{Nc}{8b}\right)\left(\frac{V_R}{V_\infty}\right)^2 [C_L \cos\beta - C_D sm\beta]$$

Denoting the right hand side of the above equation as G where

$$\varphi = \left(\frac{NC}{8b}\right)\left(\frac{V_R}{V_\infty}\right)^2 [C_L \cos\beta - C_D sn\beta] \quad (9)$$

Hence, we can write:

$a = G - a^2$ (10)

Equation 9. forms the basis for an iterative solution of the streamtube momentum equation. The function G is a rather complex function of "a" making an explicit solution for "a" not possible. The procedure for carrying out computations on a specified streamtube begins by setting "a" equal to zero. The angle of attack to the blade element can be calculated from

$\alpha = \theta - \beta$ (11)

where:

$$\beta = \arctan\frac{V_\infty (1 = a)}{V_1} \quad (12)$$

and θ is the blade element angle with reference to y axis.

The non-dimensional functions G is next competed from Equation 9.Using the present value of "a" and G in the right had side of Equating 10,anew value of "a"can be computed. The value of V/V_∞can be obtained from Equation 2.The process is repeatedThe non-dimensional functions G is next computed from Equation (9). Using the present value of "a" and G in the right hand side of equation (10). A new value of "a" can be computed. The value of can be obtained from equation (2). The process is repeated starting with the calculation of α until the desired accuracy in "a" is obtained.

The process yields the value of $V/V_\infty$for the streamtube. Normally, the convergence is rapid.

THRUST, SID FORCE AND POWER

Once the streamtube momentum equation has been solved, thrust , and side force produced and hence power spent by the blade element as it passes through the streamtube can be obtained by:

Once the streamtube momentum equation has been solved, thrust, thrut, and side force produed and hence power Sent by the blade element as it passes through the streamtube can be obtained by:

$$dT(y) = \frac{1}{2}\rho c \Delta z V^2_R(y) [C_L \cos\beta - C_D \sin\beta] \quad (13)$$

$$dF_t(y) = \frac{1}{2}\rho c \Delta z V^2_R(y) [C_L \sin\beta - C_D \cos\beta] \quad (14)$$

$$dp(y) = dF_t(y)\, V_t(y) \quad (15)$$

To obtain the total thrust, side force and

power on a wing (blade) for a particular value of y, the above quantities must be integrated or summed over the number of segments N_s making up the blade. Each blade segment is assumed to be of a length Δz. Hence; total thrust, side force and power on a complete wing are given by

$$T=\Sigma dT(y) \quad (16)$$

$$F=\Sigma dF(y) \quad (17)$$

$$P=\Sigma dP(y) \quad (18)$$

The Summation is taken over the total number of blade elements N_s

Againg , to obtain the average values produced by the system by all of the N wing, the above values must be time averaged and multiplied by N; as

$$\text{Thrust} = \frac{N}{N_t}\Sigma\Sigma dT(y) \quad (19)$$

$$F_t\text{total} = \frac{N}{N_t}\Sigma\Sigma dF_t(y) \quad (20)$$

$$\text{Power} = \frac{N}{N_t}\Sigma\Sigma dP(y) \quad (21)$$

The second sum is taken over a reasonable N_1 The total thrust, side fore and power are expressed in non-dimenal forms as:

$$K_T = \frac{\text{Thrust}}{\rho V^2_{T\max} A} \quad (22)$$

$$K_S = \frac{F_t}{\rho V^2_{T\max} A} \quad (23)$$

$$K_p = \frac{\text{Power}}{\rho V^3_{T\max} A} \quad (24)$$

where A is the total wing planform area
Hence, the system propulsion efficiency or "open water efficiency" is given by

$$\eta = \frac{Kt}{Kp} J \quad (25)$$

where $$J = \frac{V_\infty}{V_{T\max}} \quad (26)$$

The above procedure was applied to a simple one bladed, rectangular wing sculling propulsion system having the following particulars:
Wing chord = 1 m
Wing span = 8 m
Free stream velocity = 8 m/s
Wing semi stroke ratio b/c = 10
Wing profile NACA 0021
The performance was evaluated for a number of blade setting angles from 50 to 85 degrees at 5 degree interval. Lift and drag data for the profile used was taken from Refiners. 6. The data covers a full range of incidence (0 through 180 degrees) and Reynolds number from 10^4 to $5x\,10^6$ The tabulated data for a number of tested airfoil sections were stored by the author in computer input files and a two dimensional interpolation scheme was devised to interpolate for lift and drag coefficients at any given angle of incidence and Reynolds number combination. A sample of these data is shown in Figure Focus was made on the region of incidence which manifests Reynold number dependence.

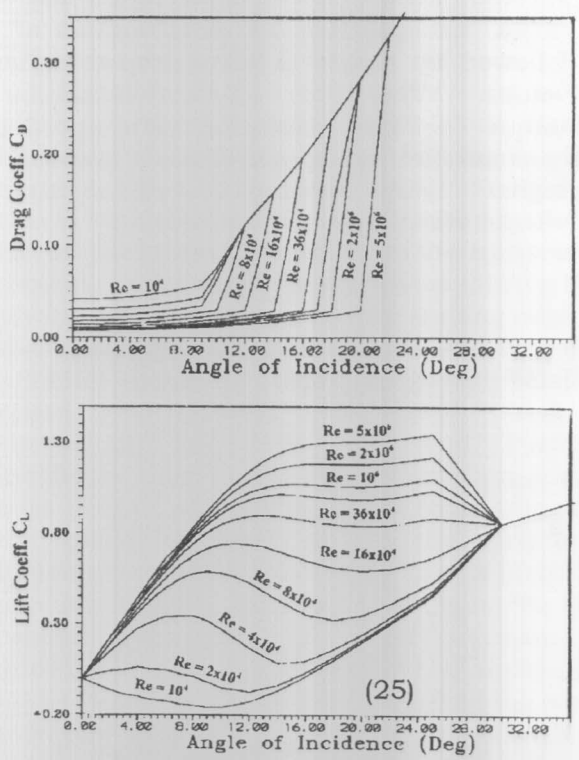

Figure3 Lift and drag characteristics of NA0021 profile

RESULTS AND DISCUSSIONS

Thrust given in a non dimensional form KT versus advance speed coefficient J for different wing setting angles is shown in Figure 4 Maximum thrust coefficient increases with the increase of both advance speed coefficient and blade setting angle. The range of speed at which the wing is developing thrust or the "operating range " gets larger as the blade angle increases. Thrust curve is a bit different from conventional propeller K_T-J curve. At low value of speed, the thrust curve is almost flat. It rises to a maximum after which it drops off linearly.

The average total side force required to move the wing expressed in a non dimensional coefficient KS is plotted against speed coefficient J for a range of blade settings in Figure 5 This force gets higher as the blade setting increases at a fixed speed coefficient. At low wing attitudes, the variation KS with speed coefficient J has a flat portion at small values of J, followed by nearly a linear drop at higher J values. This type of trend is similar to torque coefficient variation with speed of a conventional screw propeller. However, for higher wing settings the K_S-J curve is characterized by a peak value.

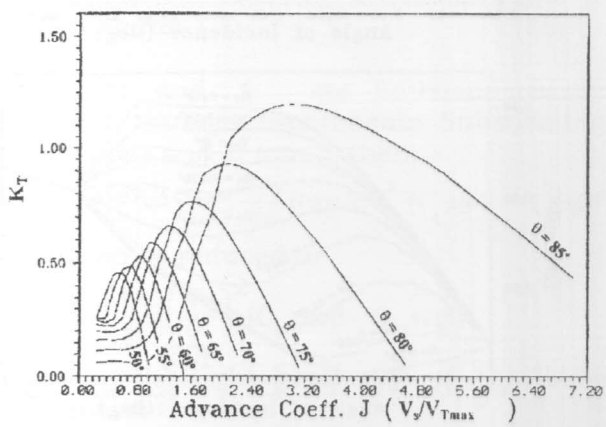

Figure 4 Thrust coefficient K_{Tt} versus advance coefficient J for different blade setting angle θ

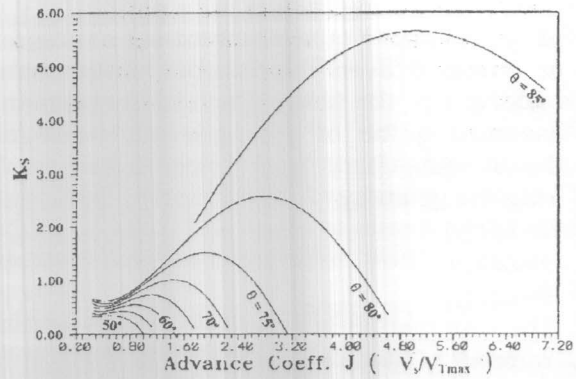

Figure 5 Side coefficient K_s versus advance coefficient J for different blade setting angle θ

The transverse force together with the blade transverse speed is used to find the power needed to move the wings. This power was also non dimensionalized as K_P and presented as function of speed coefficient J and blade setting θ in Figure 6 The power coefficient K_P curve exhibits similar trend as the K_S curve.

Performance of sculling propellers is assessed through "open water" efficiency factor that is related to K_T , K_P and J parameters. The efficiency is displayed as function of wing attitude and advance coefficient in Figure 7 For any blade setting, the efficiency increases as speed coefficient increases until a certain maximum value is reached after which the efficiency decreases to zero at the point of vanishing thrust. However, it is worth noting that the value of maximum efficiency is found to be insensitive to blade setting.

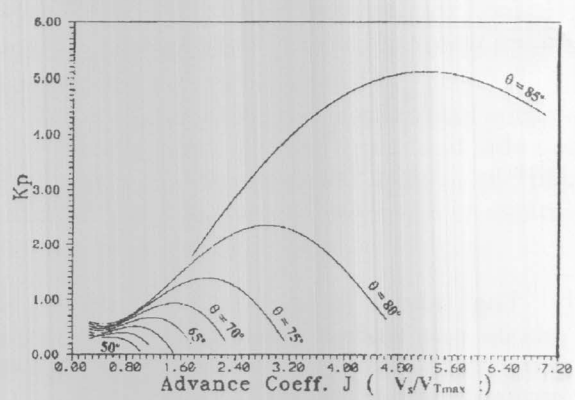

Figure 6 Power coefficient K_p versus advance coefficient J different blade setting angle θ

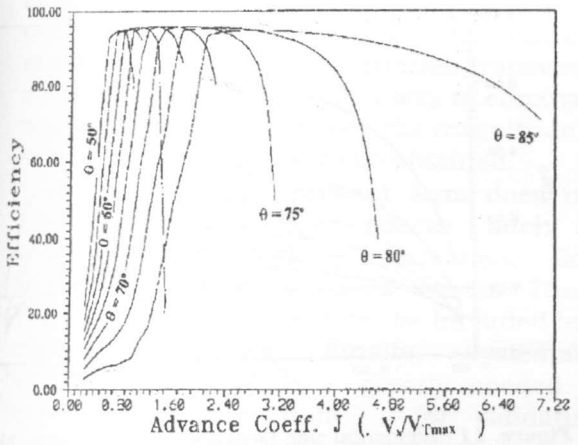

Figure 7 Open water efficiency η Versus advance coefficient for different blade setting angle θ

It is also noted that the maximum efficiency is relatively high as compared to conventional screw propellers. Analysis done by Potze [2] indicated 94 % efficiency. Blade attitude can be changed to suit different operating conditions such that maximum efficiency is attained through all range of operations. The maximum efficiency operating condition was selected for closer, or further examination. This case is taken for all blade attitudes examined. This is given in the table 1

Table 1 Maximum open water efficiency for different blade setting

Blade setting θ (degrees)	Advance Coefficient J	Open Water Efficiency η%
50	0.75	94.66
55	1	95.16
60	1.13	95.67
65	1.25	95.83
70	1.5	95.91
75	1.88	95.82
80	2.25	95.48
85	3.13	94.67

Induced velocity, flow angles, and spatial distributions of forces on the wing along its traveling path were examined in Figures 8 through (12). Axial velocity imparted to the slipstream is generally very small, that indicates light loading (the wing is lightly loaded). It was also noted that "a" is maximum at the mid stroke location, that is the position of maximum transverse speed and hence maximum inflow angles. This maximum value increases as the blong setting is reduced. Flow retardation takes place at the extreme ends of the blade stroke where the blade reverses direction; (see Figure 8).

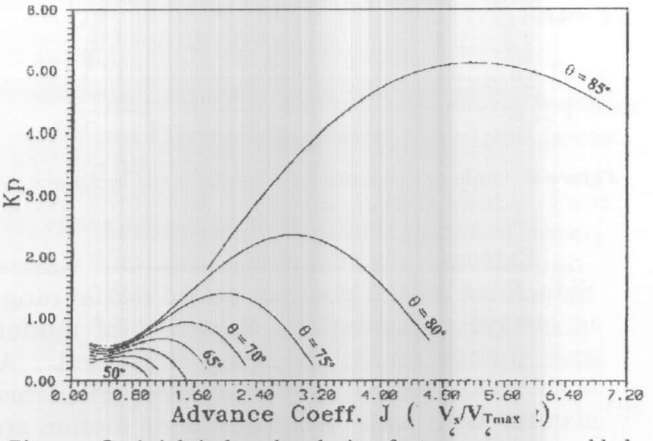

Figure 8 Axial induced velocity factor 'a' versus blade location y/b at maximum efficiency condition for different blade setting angle θ

Negative incidence to the wing takes place at the far ends of the blade stroke because the inflow angle to the wing is quiet high as the transverse speed diminishes there. Similar behavior was observed by Potze [2] at the turning points of the transverse motion of the wing. He suggested moving the pivotal points nearer to the trailing edge of the wing even though this could increase the pitching moment. Using wings with smaller chord length, (with increased risk of cavitation), are also suggested. Positive incidence and hence useful thrust produced over 90% of the wing stroke (depending on the blade settings) where the maximum incidence takes place at the midstroke position. Angles of attack to the wing for the cases studied varies between-15° and+13° . The negative range of incidence takes place at the extreme ends of the wing traveling distance where negative thrust is produced; (see Figure 9) Thrust, side force, and spent power varies al the wing stroke. Maximum values are located at mid position.

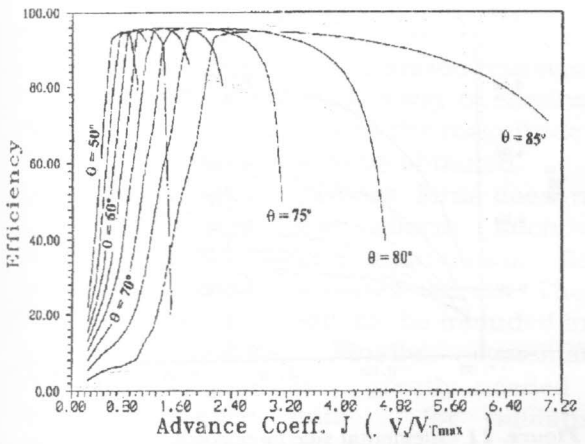

Figure 7 Open water efficiency η Versus advance coefficient for different blade setting angle θ

It is also noted that the maximum efficiency is relatively high as compared to conventional screw propellers. Analysis done by Potze [2] indicated 94 % efficiency. Blade attitude can be changed to suit different operating conditions such that maximum efficiency is attained through all range of operations. The maximum efficiency operating condition was selected for closer, or further examination. This case is taken for all blade attitudes examined. This is given in the table 1

Table 1 Maximum open water efficiency for different blade setting

Blade setting θ (degrees)	Advance Coefficient J	Open Water Efficiency η%
50	0.75	94.66
55	1	95.16
60	1.13	95.67
65	1.25	95.83
70	1.5	95.91
75	1.88	95.82
80	2.25	95.48
85	3.13	94.67

Induced velocity, flow angles, and spatial distributions of forces on the wing along its traveling path were examined in Figures 8 through (12). Axial velocity imparted to the slipstream is generally very small, that indicates light loading (the wing is lightly loaded). It was also noted that "a" is maximum at the mid stroke location, that is the position of maximum transverse speed and hence maximum inflow angles. This maximum value increases as the blong setting is reduced. Flow retardation takes place at the extreme ends of the blade stroke where the blade reverses direction; (see Figure 8).

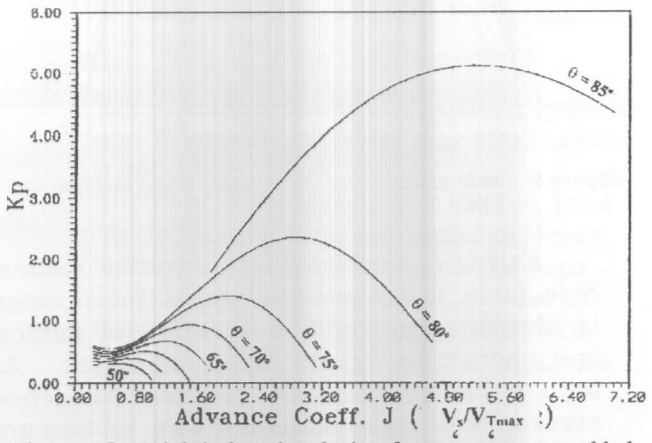

Figure 8 Axial induced velocity factor a versus blade location y/b at maximum efficiency condition for different blade setting angle θ

Negative incidence to the wing takes place at the far ends of the blade stroke because the inflow angle to the wing is quiet high as the transverse speed diminishes there. Similar behavior was observed by Potze [2] at the turning points of the transverse motion of the wing. He suggested moving the pivotal points nearer to the trailing edge of the wing even though this could increase the pitching moment. Using wings with smaller chord length, (with increased risk of cavitation), are also suggested. Positive incidence and hence useful thrust produced over 90% of the wing stroke (depending on the blade settings) where the maximum incidence takes place at the midstroke position. Angles of attack to the wing for the cases studied varies between-15° and+13° . The negative range of incidence takes place at the extreme ends of the wing traveling distance where negative thrust is produced; (see Figure 9) Thrust, side force, and spent power varies al the wing stroke. Maximum values are located at mid position.

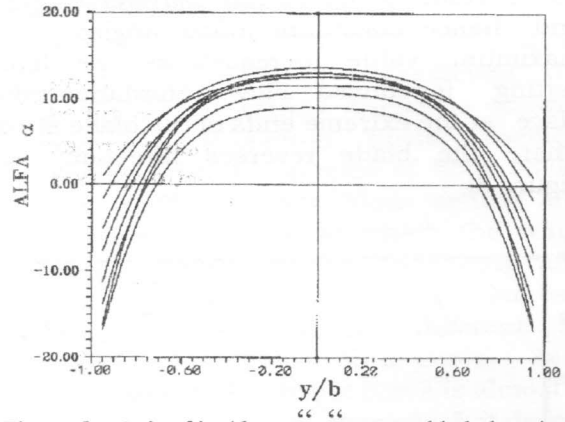

Figure 9 Anle of incidence " α " versus blade location y/b blade setting angle

Extreme ends exhibit negative values. Side force at the positive useful thrust range is always opposing the direction of motion and, hence energy is being expended. At both stroke ends where negative incidence occurs, both side force and wing motion are in the same direction so, energy or power is produced or "generated" there; (see Figures 10,11, and 12). This type of plots is quite useful as a starting point for eliminating or reducing the reverse thrust part during the cycle of operation. This will be achieved through synchronized angling of the blade with transverse blade motion. Another angling scheme could be devised such that the average side force could be minimized. As such, the most efficient flapping motion can be programmed.

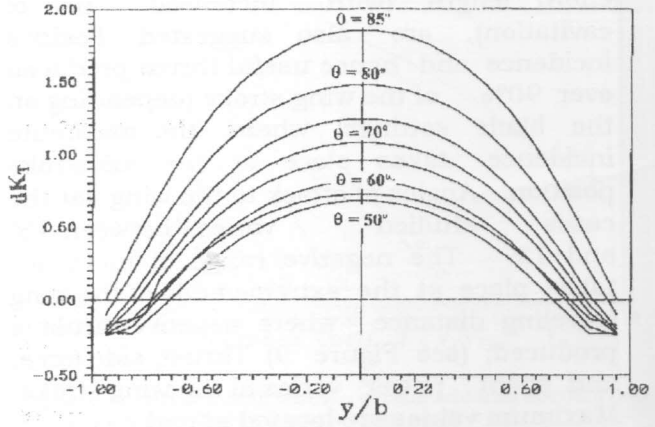

Figure 10 Elemental thrust coefficient dk_T versus blade location ylb at maximum efficiency condition for different blade setting angle θ

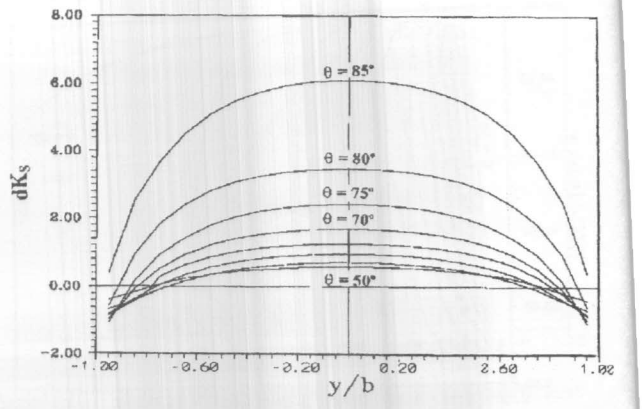

Figure 11 Elemental side force coefficient dk_s versus blade location y/b at maximum efficiency condition for different blade setting angle θ

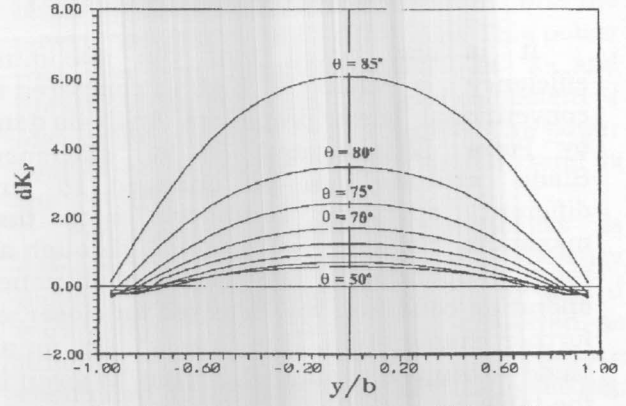

Figure 12 Elemental power force coefficient dk_T versus blade location y/b at maximum efficiency condition for different blade setting angle θ

CONCLUDING REMARKS AND RECOMMENDATIONS

The simple preliminary analysis done on a sculling propulsion system indicates a quite promising performance. Higher efficiency, as compared to conventional screw propellers was attained. The analysis has separated angling motion from transverse blade motion to provide a tool to assess the effect of each on the overall efficiency. Performance efficiency at part and/or overloads can be improved through changing blade angle during operation making use of the spatial variation charts of axial and side force. The analysis can also be used to study the effects of some important geometrical parameters on the hydrodynamic performance. These parameters include number of wings, profile type, aspect ratio, wing platform, and taper

ratio. A number of blade motion kinematics can also be tested through the current analysis. Devising synchronized transverse and blade angling in such a way to eliminate negative thrust or to reduce the magnitude of side force values may also be obtained.

The analysis in its present form does not handle unsteady flow effects such as dynamic stall, wake deformation, flow separation, and tip vortex effects. These real flow aspects need to be included in a modified analysis. Finally, systematic experimental work is greatly needed to provide reference data for validating different analysis tools. Interaction between wings and hull, wing cavitation, and noise and vibration levels need also be experimentally investigated.

REFERENCES

[1] Robert Taggart, "Marine Propulsion : Principles and Evolution", Gulf Publishing Company, Houston, Texas, 1969.

[2] W. Potze, "On Optimum Sculling Propulsion"; Journal of Ship Research, Vol. 30, No. 4, Dec. pp221 -241. 1986

[3] J. A. Sparenberg, and Vries, J. de, "On Sculling Propulsion by Two Elastically Coupled Profiles"; Journal of Ship Research, Vol. 27, No. 2, June pp. 135-146, 1983.

[4] J. A .Sijtsma and Sparenberg,. "On Useful Shapes of Rigid Wings for Large Amplitude Sculling Propulsion"; Journal of Ship Research Vol. 36, No. 3, Sept. pp. 223-232, 1992.

[5] "Propulsor Efficiency:MIT Penguin Boat Takes Maiden Voyage", Maritime Reporter and Engineering News, May 1997 Issue , p 36.

[6] Sheldahl, E Robert. and C Klimas, Paul "Aerodynamic Characteristics of Seven Symmetrical Airfoil Sections Through 180-Degree Angle of Attack for use in Aerodynamic Analysis of Vertical Axis Wind Turbines", SAND80-2114, Sandia National Laboratories, 1981.